

Empirical Analysis of Multiwalled Carbon Nanotube Deposition for Enhancing Mechanical and Tribological Characteristics in Aluminium-Based Metal Matrix Composites

Vikram K Vasu¹, Umashankar K S², Vijay Kumar S^{1*}

¹Department of Mechanical Engineering, Nitte Meenakshi Institute of Technology, Visvesvaraya Technological University, Bengaluru, Karnataka

²Department of Mechanical Engineering, KVG College of Engineering, Visvesvaraya Technological University, Sullia, Dakshina Kannada, Karnataka

Received 26 Apr 2023

Accepted 27 Aug 2023

Abstract

Utilizing Laser Engineered Net Shaping (LENS), nanocomposites were generated by mechanically combining metal powders with various amounts of multi-walled carbon nanotubes (CNTs). To produce free-standing bulk structures and coatings, the LM6 (Al-12Si-0.6Fe-0.5Mn-0.3Mg-0.1Ni-0.1Zn) alloy was chosen owing to its exceptional corrosion resistance in typical atmospheric and marine environments. The LENS technique was employed to fabricate the coating-substrate interface for LM6 coated Al-2024 and MWCNT-LM6 coated Al-2024. The addition of MWCNTs to the Al-Si matrix enhanced the tribological properties of LM6. SEM images revealed abrasive wear as the primary wear mechanism. A pin-on-disc wear tester was utilized to study the friction and wear behavior of the composite under a load of 1 N and a sliding speed of 50 mms⁻¹. The addition of MWCNTs resulted in a reduction of the friction coefficient because of the MWCNT's self-lubricating characteristic and unique topological structure. Moreover, the volumetric wear rate dropped considerably, and thermal properties were significantly enhanced with the inclusion of MWCNTs. A 25% increase in thermal conductivity was seen after the addition of 8% vol MWCNTs to LM6 coated Al-2024.

© 2023 Jordan Journal of Mechanical and Industrial Engineering. All rights reserved

Keywords: LM6; MWCNT's; Al2024; Wear; Thermal Conductivity; Coating.

1. Introduction

Metals and alloys are very popular as structural materials. Some metals and metal alloys per unit mass have high structural strength, making them useful materials for bearing large loads or resisting damage to impacts. It is also possible to engineer metal alloys to have elevated shear, torque, and deformation resistance [1]. The strength of metals and metal alloys can be improved by heat treatment to a certain extent. The progress in the development of MMC's has led to more studies that further escalated the stiffness and strength of the metal. The strength and ductility associated with MMC's are added by the metal matrix and reinforcement that is either high rigidity metal or ceramics based on a particular matter or fiber offers further improvement in strength and/or stiffness [2]. High Thermal Conductivity and low thermal expansion coefficient characteristics can be engineered into metal matrix composites that can make MMC's idyllic for a number of applications, including electronic packaging [3].

The excellent physical properties of multi-walled carbon nanotubes (hereafter referred to as MWCNTs, unless indicated) make them an attractive candidate for use as reinforcements in metal matrix composites [4]. However, there has been little progress in this field compared to polymer-based

nanocomposites which can be credited to the relative ease with which polymer-based composites can be processed, which often does not require any high processing temperatures. In recent years, various research groups have begun to focus on the processing of MWCNT reinforced MMCs [5-7]. Because of their high specific strength, these composites are intended for use in structural applications as well as using materials because of their exciting thermal properties. This study focuses on the use of Laser Engineered Net Shaping (LENS) for MWCNT-MMC manufacturing. Lasers are attractive production tools because they deliver a range of unique benefits, such as high efficiency, automatic reliability, non-contact production, finishing operations elimination, reduced processing costs, enhanced product quality, increased use of material, and minimal heat affected area [8-12]. Laser processing technology can be used to deposit metals and alloys with fine grain microstructure using appropriate operating parameters [13-16]. It can be used to build parts with good mechanical properties. The motivation of this study was to explore the possibility of using LENS to process MWCNT-MMCs. The combination of LENS processing with MWCNT reinforcements can help in the development of high-performance engineering materials. In this study, MWCNTs were used to reinforce Al-12Si alloys. The microstructure and

* Corresponding author e-mail: vijaysnitk@gmail.com.

some physical properties such as thermal and mechanical properties of these composites have been studied.

Laser Engineered Net Shaping is capable of producing parts that are near net shape and require little post-processing or machining. The LENS (Figure 1 [17]) consists of a laser Nd: YAG continuous wave, a controlled atmosphere glovebox, a positioning device controlled by the x-y-axis computer, and a powder feed unit/unit. Inside the argon-filled glovebox, the positioning stage is mounted, functioning at a marginal oxygen level of 2-3 parts per million. Through a window mounted on the top of the glovebox, the laser beam is brought into the glovebox and guided using a plano-convex lens to the deposition area. The machine is equipped with a powder feed unit or units that supply powders for the materials being deposited. The powders are fed into the unit and supplied through a multi-nozzle assembly via flowing argon. The nozzle assembly is designed to converge the powder stream on the laser beam, which is centered on the substrate. The substrate is mounted on a positioning device to ensure precise control during the deposition process. [17-19].

The laser power level, powder feed rate, scan speed, and hatch/raster spacing are all processing parameters in the LENS technique [20-26]. Depending on the material being deposited, these process parameters are adjusted. When depositing materials with high laser absorptivity, for example, laser power is reduced, while materials with low laser absorptivity need a higher laser power level. The substrate that is chosen influences the bonding between the deposited element and the substrate. Powder flowability is critical for LENS manufacturing, and good flowability is required. Clogging in the powder delivery system can be caused by poor powder flowability. Microstructure, surface finish, hardness, and size can all be regulated by choosing the right process parameters. Since the LENS process requires rapid solidification of molten metal, the deposited sections may have a fine-grained microstructure. As a result, as expected by Hall-Petch strengthening, better mechanical properties can be achieved when compared to traditional melting and solidification paths. The processing conditions can be changed to choose various microstructures and to take advantage of all the advantages of metastable microstructures. Since the deposition is done in an argon environment, oxidation issues during processing can be avoided. LENS' ability to handle compositionally and functionally graded materials is a key feature. This method can

generate metallic structures directly from CAD data, which cuts down on processing time and eliminates the risk of human error. Finally, LENS can produce complex near-net shape structures that does not require surface finishing [27-28].

The exceptional physical properties of multiwalled carbon nanotubes (MWCNTs) have generated considerable interest. Through extensive experiments and simulations, it has been demonstrated that MWCNTs possess high stiffness (~1000 GPa) and yield strength (~100 GPa) in the direction of the tube length [29-31]. Their low density also makes them suitable for use in lightweight, high-strength applications, including aerospace components. Additionally, MWCNTs exhibit high thermal conductivity (ranging from 2750 W/m-K to 5890 W/m-K along the tube axis) and a negligible coefficient of thermal expansion (~ 0×10^{-6}) [32-33], making them highly desirable for thermal management applications. Furthermore, MWCNTs are thermally stable up to 2750°C in a vacuum [34-36]. To ensure uniform distribution of MWCNTs in aluminum, the melt infiltration technique was employed [37]. Melt infiltration techniques use a solid porous structure in which MWCNTs are dispersed. The molten metal (matrix) is then infiltrated into the pores and allowed to solidify. Due to the high temperature of the molten metal, the solid perform can melt leading to agglomeration of MWCNTs. Also, the time required to fill the porous, solid perform and efficiency of the processes are other critical factors that decide the final properties of the composite in this case. However, improved dispersion has been reported for Al-MWCNT [38-43] and Mg-MWCNT composites. As compared to powder metallurgy, the melting techniques should ideally produce much denser composites. The interfacial bonding would depend on the wettability of MWCNTs with the matrix. The formation of MWCNT clusters and interfacial compound formation should be preventable by using rapid solidification techniques.

Based on the previous work, adding MWCNT with the metal matrix composites plays a vital role in many applications. The researchers discussed the different compositions with base metals to study the behaviour of mechanical properties. This study focused on coating of MWCNT on LM6 alloys for different composition to study the performance of thermal conductivity and wear behaviour. This investigation gives a better understanding of thermal conductivity for different composites and compares the results with wear rate of the developed samples.

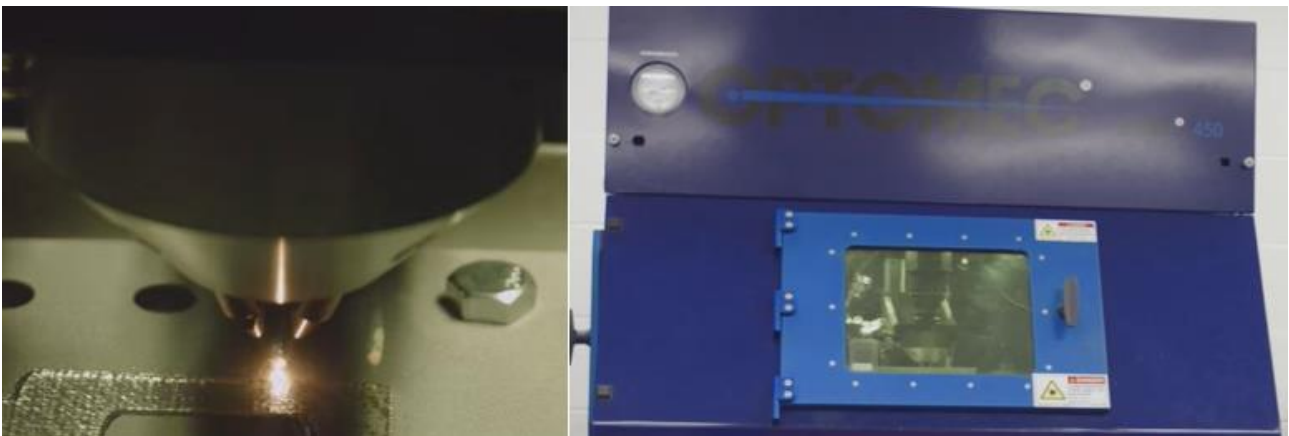


Figure 1. [17]: The Arrangement of Laser Engineered Net Shaping (LENS) is depicted: 1. Power Supply; 2. Pneumatic Pulsating System; 3. Visual System; 4. IPG Fiber Laser; 5. Mainframe Control; 6. Data Input; 7. Working Cavity; 8. Laser Optical Pathway; 9. Functioning Head with Nozzles (Four); 10. Statistically Guided Working Counter (Motion in Plane of X-Y); 11. Antechamber.

2. Materials and Methods

The LM6 (A413 Alloy) powder (99.9% pure, -140+325 mesh, melting point ~ 6500C, supplied from Fenfee Metallurgy's) and Multi-walled MWCNTs (95% pure, 30-50 nanometers in outside diameter, and a length ranging from approximately 10-20 μm , supplied form Adnano Technologies) was used as preliminary materials for preparing MWCNT-Al-Si composites. The ratio of LM6 powder added in the volume percent of 92% (149.2 grams) for the 8% of MWCNT's (0.80 grams). Figure 2 (a), (b) and (c) illustrate the powder form of MWCNT with surface morphology of LM6 as the matrix material for the fabrication of the composite with EDS analysis of the composites.

Table 1. Properties of Multi Walled Carbon Nano-Tubes

Properties	Values
Purity	Carbon >99%
Average Length * Diameter	1-5 μm * 10-15 nm
Strength	10-60 GPa
Surface Area	370 m ² g
Melting Point	3645-3702 °C
Density	~2.1 g/ml at 25 °C

2.1. Wear Test

Many methods were used to measure the wear [51-60] in compliance with ASTM G133, wear testing was conducted on the test samples (unreinforced LM6 and 8 vol% MWCNT-LM6 coatings on Al-2024 substrate) using a tribometer with a 6 mm diameter chrome steel ball. The wear test was a rotating pin-on-disc test carried out at a load of 25 N, a frequency of 5 Hz, a stroke of 10 mm, and test durations ranging from 40 s to 16 min. The wear test samples had a diameter of 15 mm and were produced using LENS. Standard metallographic preparation procedures were followed to obtain a flat surface and good surface finish by polishing the samples. Two samples were prepared for each composition. The pin used in the test had a 6 mm radius end. Two different tests were performed on each sample with wear track radii of 2mm and 4mm (full rotation represents 12.5mm and 25mm of travel respectively) at a speed of 2500 rpm. The total distance travelled by the rotating pin for tests with a wear track radius of 2mm was 1000m and the total time taken was 7 hours. The total distance

travelled, and time taken was 3000m and 20 hours respectively for the wear tests performed with a 4 mm wear track radius. Prior to each test, the specimens and the chrome steel ball underwent a cleansing process using 100% ethanol to guarantee the cleanliness of their surfaces. The wear tests were performed under arid conditions at ambient temperature. A normal load of 1 N was used for all tests. After performing the wear test, the samples were ultra-sonicated for 10 minutes and then examined using SEM. A MG-2000 high-speed, high-temperature pin-on-disc wear machine was put through wear testing in an unlubricated sliding environment at standard optimum temperature of 21 to 24°C with 50 to 60% relative humidity was maintained. An analogous wear method was followed by numerous researchers [44-45].

2.2. Thermal Conductivity

The technique of laser or light flash is commonly used to measure the thermal diffusivity of various materials. This method involves the application of a light pulse on the front surface of a plane-parallel sample, causing it to heat up. The temperature rise at the back face of the sample is recorded over time, and materials with higher thermal diffusivity exhibit a faster temperature increase at the back face. Pure LM6 and 8vol% MWCNT-LM6 samples were polished so that they would have the same surface roughness on the coating side as well as the substrate side. Thermal diffusivity and specific heat were measured b/w 250C-2500C using LFA 447 nano flash which uses the flash method as per ASTM-E1461-07. Two samples were tested for each composition. Initially, a thermal conductivity test was conducted to evaluate the integrated structure of the substrate and coating as a single layer. To avoid laser light and the generation of plasma on the surface, the samples were coated using a carbon spray on the top and bottom surfaces. Five tests were conducted on each sample to obtain accurate results and the mean value was used for calculations. Subsequently, a double layer test was conducted to evaluate the thermal conductivity of the coatings and the thermal contact resistance at the interface. To determine the thermal contact resistance, Proteus LFA analysis software was fed with thermal diffusivity and specific heat capacity values for pure LM6 and Al-2024.

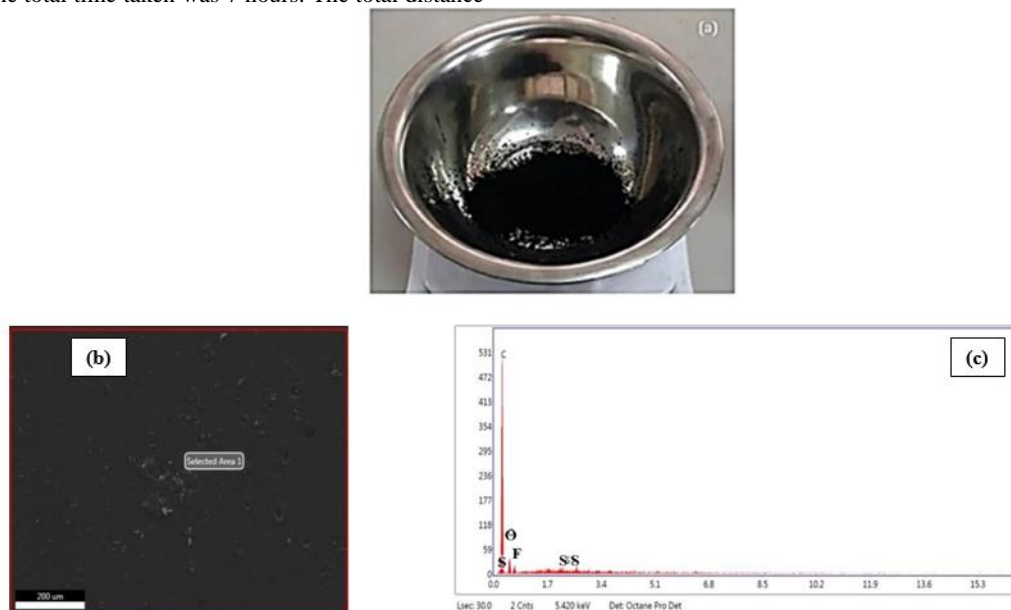


Figure 2. (a) Multi-Walled Carbon Nanotubes Powder (b) EDS micrograph of LM6 Alloy of Specimen (c) EDS spectra of the Specimen

3. Results and discussions

3.1. Surface morphology of the samples

The morphology of silicon within the eutectic phase is the most crucial microstructural attribute in aluminum-silicon eutectic alloys. The alteration of the silicon structure in the eutectic is an important method to enhance the strength of the alloy. Silicon in the eutectic phase can exhibit different microstructures, including unmodified (large acicular, rod, angular, faceted, flake), partially or completely modified (modified angular, fibrous), or over-modified (massive, acicular, rod, angular, faceted, flake). The Eutectic Al-Si alloy (12.25 percent Si) solidifies at a single temperature. This alloy is frequently used in the production of heavy-duty diesel pistons, pulleys, sheaves, and other automotive components. To understand how unmodified and over-modified silicon work, researchers analyzed and compared the composition of the eutectic silicon phase in both unmodified and silicon-modified alloys.

The research utilized Aluminum Powder to conduct SEM/EDS tests, which were analyzed using the automated feature analysis (AFA) program as displayed in figure 2. Small particles, known as very small particles (VSP), are often overlooked in forensic science despite being common in our surroundings. Their size varies significantly, even below typical trace evidence. The SEM is a scientific instrument that utilizes electrons instead of light to generate highly magnified images. The microscope consists of an electron gun positioned at the top, which produces an electron beam. The microscope is maintained under a vacuum, and the electron beam penetrates the sample in a vertical direction, resulting in the production of an image.

A pre-existing technique was used, with a combination of seldom seen and frequently seen elements. The SEM/EDS or the program may not limit the number of elements (among those observables by EDS), and the element assortment can be modified. The number of elements chosen influences the overlap of x-ray lines, but ambiguities are overcome by using known associated x-ray emissions for the same elements by the x-ray detection program. Carbon nanotubes (CNTs) are nanomaterials consisting of carbon atoms. This research focuses on multi-walled carbon nanotubes (MWCNTs) as they have significant relevance to industry, as illustrated in Figure 3. MWCNTs are cylindrical structures made of multiple layers of graphite that are rolled inward. MWCNTs exhibit remarkable properties, including electrical conductivity equivalent to copper, exceptional mechanical strength, withstanding 15 to 20 times more force than steel despite being only 5 times lighter. Furthermore, MWCNTs have high thermal conductivity, comparable to copper, and exceeding

diamond's thermal conductivity by over five times. These features make MWCNTs an attractive option for various industry applications.

Carbon nanotubes with multiple walls are formed in a helix shape, wrapping around one another. About 80% of the CNTs contain a helical configuration. The rest are typical CNTs. The majority of the CNTs have an outer diameter of 100-200 nm, and the total CNT concentration is greater than 90% by weight. A layer of carbon atoms that are linked together in a hexagonal (honeycomb) mesh create the structure of a carbon nanotube. Graphene is a single-atom thick layer of carbon that is coiled into a cylinder shape and joined together to form a carbon nanotube. In Fig 4(a), X-ray diffraction (XRD) patterns were obtained for the multi-walled carbon nanotubes (MWCNTs). The pristine MWCNTs displayed two peaks, one at the 002 and 001 plane, and the other at the 101 and 200 plane, with an interplanar spacing of 3.41 Å and 2.05 Å, respectively. It is evident from the Figure that functionalization of the MWCNTs did not modify the crystallographic properties of the MWCNTs as they still had only two prominent peaks. The LM6, on the other hand, exhibited a slightly different pattern, which may be due to the high degree of functionalization in this study.

From the XRD Profile for Multi-Walled Carbon Nanotubes, for a position angle ($2\theta = 26^\circ$), the peak is observed in XRD Plot with the number of counts exceeding 4000 in the bandwidth of 0 degrees to 90-degree phase shift. This is basically attributed to the spiral nature of the multi-walled carbon nanotubes and their helical structure. FESEM images of as-grown CNTs after the CVD phase at 550°C are shown in Figures 5 (a) and (b). Figure 5(a) depicts the as-grown CNTs' overall surface morphology, which appeared thick, entangled, and noodle-like. The CNTs had a rough tube surface, as shown in Figure 4 (b). The presence of open ends tubes in some of the CNTs suggests that the CNTs' growth mechanism is a tip-ripping model. The results show that the BWH acted as a pore and active site for anchor catalyst particles in the CNT synthesizing process.

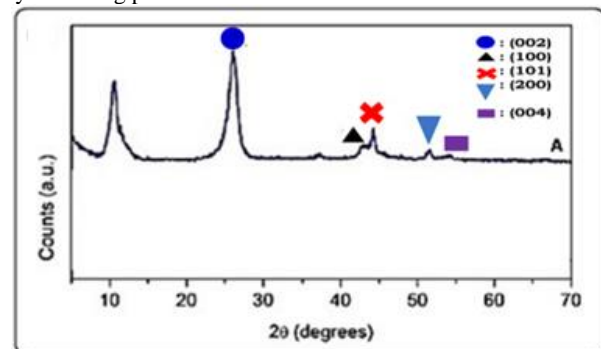


Figure 3. XRD profile of as received multi-walled carbon nanotubes.

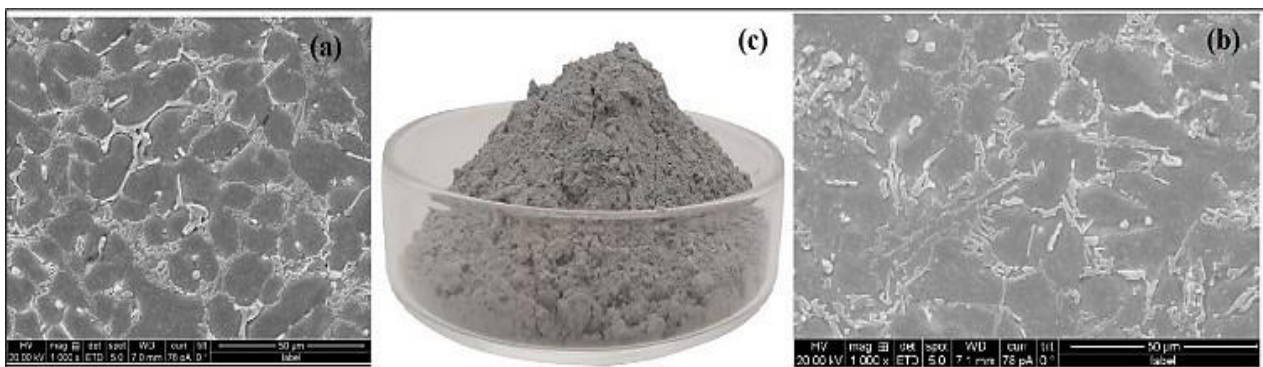


Figure 2. (a) & (b) SEM images of LM6 Powder and (c) LM6 Powder

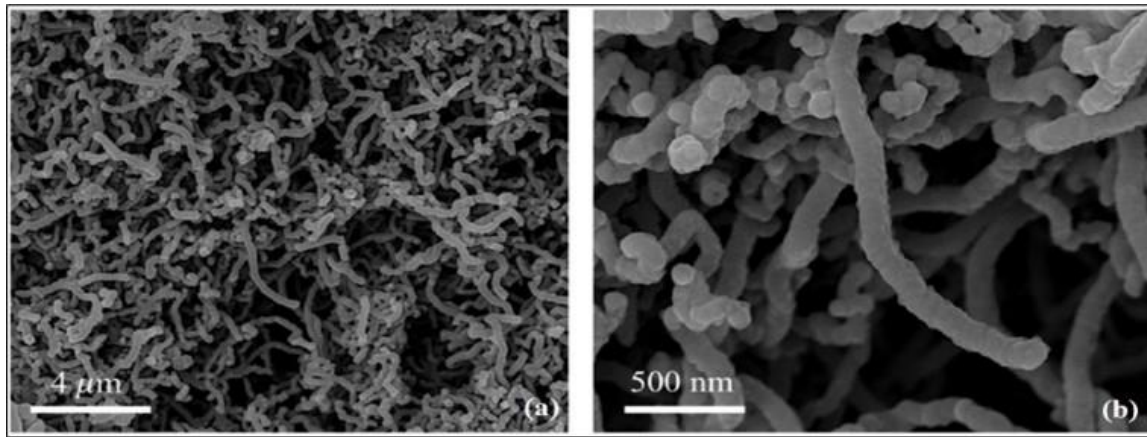


Figure 4. FESEM images at various magnifications: (a) low magnification of compact and intertwined as-growth CNTs after CVD at 550°C, and (b) high magnification of as-growth CNTs' surface structure.

To disperse MWCNTs in LM6 powder, ball milling was employed. A metallic container was used to hold 149.2g of LM6 powder with 8 vol. % of MWCNTs and 100 steel milling balls, each with a diameter of 6 mm (initial ball to powder ratio of 1:1.5). To prevent cold welding of MWCNTs on steel balls and the container, a control agent, Methanol (6 vol %), was added. The container was then placed on a ball mill, and its contents were mixed for 24 hours at a speed of 60 rpm. Laser deposition was performed on an aluminum substrate (Al-2024, T-6) at two different power levels: 500W and 250W. A scan speed of 35 mm/s and a powder feed rate of 5.25 g/min were used.

Coatings with 12 mm and 15 mm diameter were deposited to perform wear test and thermal conductivity test respectively. Coating thickness was guided by the number of layers deposited on the substrate and, after grinding and polishing, 0.25 mm thick coatings were obtained. A computerized reading of the impedance change serves as a gauge for coating thickness. Eddy-current monitoring of coating thickness is a commonly used technique for liquid or powder coatings on aluminum, non-magnetic stainless steel, and anodized aluminum. It is crucial to ensure that thinner measurements confirm the removal of the clear coat or the readiness of the primer to show through by verifying the impedance. In an argon atmosphere, laser deposition was performed to prevent MWCNT loss at high temperatures. Samples generated at 250 W showed severe balling and were not used for analysis. Coatings produced at 500W were polished to obtain a smooth surface. Using the same parameters, pure LM6 coatings were also deposited on an Al-2024 substrate.

Coating Multi-Walled Carbon Nanotubes (MWCNT) onto LM6 involves a step-by-step process to ensure successful integration and desired properties. First, begin by dispersing MWCNT in a suitable solvent, such as isopropyl alcohol (IPA) or a combination of solvents. Then, ultrasonicate the mixture to ensure proper dispersion and break up agglomerates, resulting in a uniform suspension of MWCNT. Next comes the preparation of surface of the LM6 by cleaning the surface of LM6 using appropriate cleaning agents to remove contaminants, oxides, and oils, ensuring good adhesion of the MWCNT coating. Apply a primer or a binding layer onto the LM6 surface to enhance adhesion between the substrate and the MWCNT coating. This layer can improve the durability of the coating. Ensure an even and controlled application to prevent excessive build-up and ensure uniform coverage. Finally, allow the coated LM6 to air-dry or use controlled

heating to facilitate solvent evaporation. The coated LM6 to a controlled temperature (annealing) process in an inert or reducing atmosphere. Annealing helps to enhance adhesion, remove residual solvents, and improve the structural integrity of the MWCNT coating.

Scanning electron microscopy and optical microscopy were used to examine the microstructure of the coatings. To reveal the microstructural features, the polished samples were treated with a solution consisting of 2.5 ml of HF (40%), 3.5 ml of Hydrochloric Acid (35%), 5.5 ml of Nitric Acid (70%), and 250 ml of distilled water. The microstructural examination was performed on the cross-section of the samples. Direct Laser Deposition (DLD) is an additive manufacturing (AM) technique that involves selectively depositing powder and melting it simultaneously with a laser beam to generate a molten pool on the substrate. The product is produced by selectively melting a sequence of powder layers using the laser beam. If the powder is exposed to radiation and provided with enough power, it will melt to create a liquid pool.

3.2. SEM analysis of MWCNT composites

Figure 5 (a) and (b) shows the SEM micrographs of the top surfaces of the LENS fabricated LM6 and MWCNT-LM6 composite coatings. MWCNTs are seen in Figure 6 (b), which is the SEM image of the MWCNT-Al-Si coating. The micrographs mainly show -Al (dark grey phase) and Si (light grey phase). During processing "balling" effect was observed in the MWCNT-LM6 composites. In LENS, a laser beam scans the composite surface line by line, inducing melting along a row of powder particles and producing a cylindrical track of molten material. When this cylinder breaks apart into a row of spheres to minimize the surface area, agglomerates arise. Balling led to the formation of porosities in the composite coating as seen in Figure 6. Figure 7 shows the optical micrographs of the coating-substrate interface for both LM6 coated Al-2024 and MWCNT-LM6 coated Al-2024. However, MWCNT-LM6 composite coatings showed more porosity owing to the balling effect. The issue of wetting between liquid metal and solid surfaces is one of the causes of balling. That is, if a liquid drop does not spread out after contacting a smooth, homogeneous solid surface, a liquid drop will be created. The balling effect can be avoided by reducing the thickness of the powder layers, slowing down the scan speed, and increasing the process's power input [46].

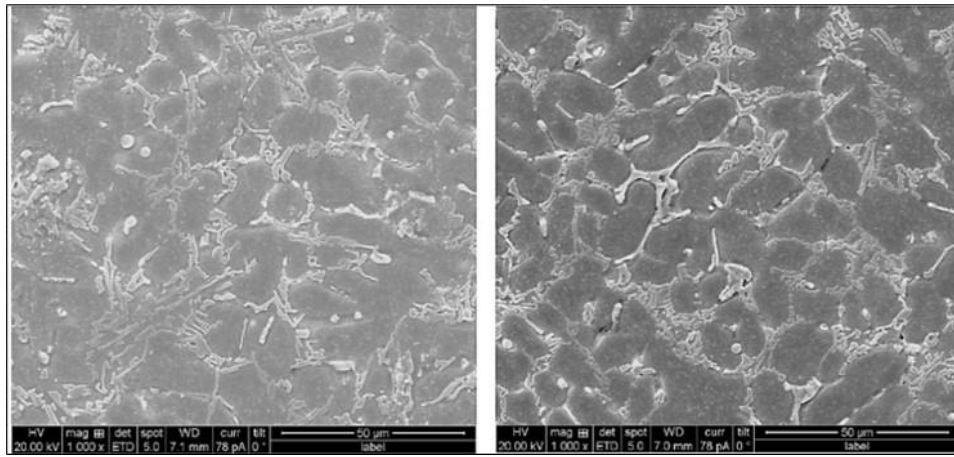


Figure 5. SEM micrographs of polished surfaces of (a) LM6 coating (b) MWCNT-LM6 composite coating

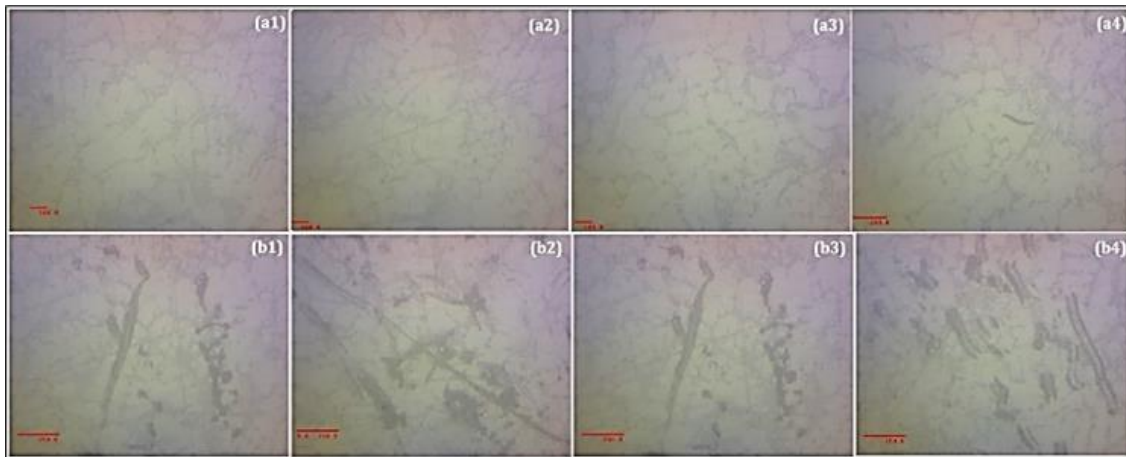


Figure 6. Optical micrographs of surfaces of (a) LM6 coating (b) MWCNT-LM6 composite coating

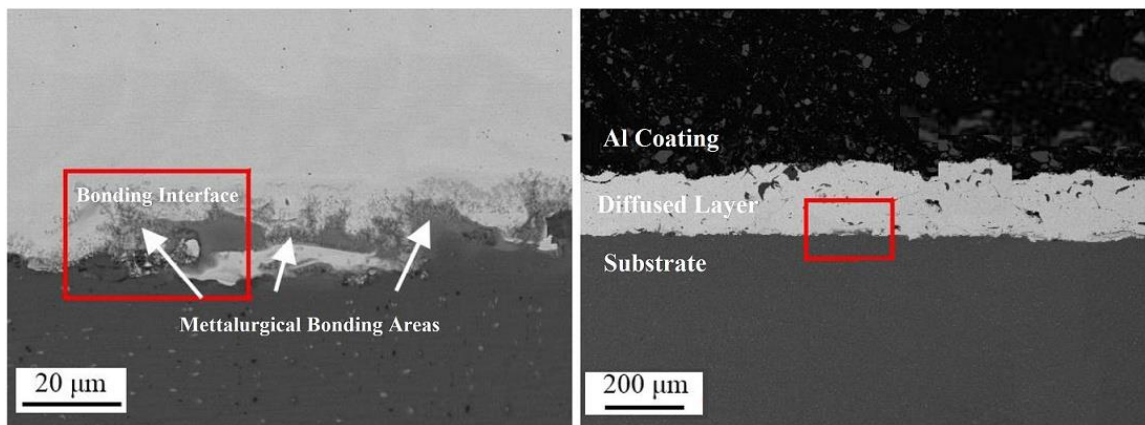


Figure 7. Optical Micrographs of coating-substrate interface for (a) LM6/Al (b) MWCNT

In general, the volumetric wear rate of a material is expected to increase first and stabilize after a certain distance is travelled by the rotating pin in contact with the surface. However, in this case, the wear rate for a total path distance of 3000 m is greater than the wear rate for a total path distance of 1000m. This means that the wear rate was still increasing and had not reached a steady state yet. The limitations imposed by the thickness of the coatings did not allow to determine the steady-state wear rate. The coefficient of friction for unreinforced LM6 coatings seems to increase in the beginning. This is because of the presence of surface porosities which increase the surface roughness, hence increasing the coefficient of friction. A similar spike can be seen for the 8-vol%-MWCNT-LM6 coating as well. The coefficient of friction for the LM6 coating and MWCNT-LM6 after travel of 1000m was

0.35 and 0.21 respectively. The coefficient of friction did not show appreciable change afterward and after 3000m of travel, the values were 0.39 for LM6 coating and 0.22 for MWCNT-LM6 coating. The average coefficient of friction was 0.19 for MWCNT-LM6 coating which was lower than that for LM6 coating (0.36). It has been reported in the literature that the presence of MWCNTs near or on the surface of the MWCNT-reinforced MMCs reduces the direct contact between the matrix and the steel ball. Due to the self-lubrication of MWCNTs, these tubes shaped reinforcements can roll or slide between the bodies in contact. The increase in hardness of the coating surfaces due to the addition of MWCNTs is an additional factor that contributes to the increase in wear resistance [47-48].

3.3. Wear surface morphology using SEM analysis.

Figure 8 displays the SEM micrographs [61 – 66] of the wear tracks on LM6 and MWCNT-LM6 coatings. In Figure 8 (a) and (b), the wear debris accumulated on the wear track can be observed. Figure 8 (c) reveals the presence of cracks, indicating the occurrence of adhesive wear. The presence of grooves on all the wear tracks shows that wear was due to two-body abrasions, while the deformed surfaces in Figure 8(c) and Figure 9 (d) show that there was wear due to three-body abrasions. Wear due to third body abrasion could have been caused by the micro-debris produced by adhesion wear or large debris from fatigue cracking. These cracks grow up and are separated from the surface and therefore become wear debris [49-50]. The presence of micro debris from adhesion wear is seen in Figure 8 (c) and Figure 9 (c). Two-body abrasion is generally more than three-body abrasion. From the SEM images, it appears that abrasive wear is the main wear mechanism involved in the wear of these coatings. Load

transfer is complete from matrix to evenly distributed CNTs in MWCNT-Al nanocomposites. Figure 10 depicts the dispersion of MWCNTs on worn surfaces (a). To reduce wear, the CNT and matrix should be bonded together. CNTs in the matrix form a strong interfacial bond with the matrix shown in Fig. 9 (b). As shown in Fig. 9 (c) and (d), MWCNTs at the granule boundaries act as a wear barrier by preventing crack growth and bridging grain boundaries. Delamination is exacerbated if the applied load is excessive. The greater the applied load, the wider the wear scratches become. At low and high loads, the worn surface is rough and soft. Compared to other materials, these composites had a softly worn surface. Due to the solid lubricant coating growing on the specimen's worn surface, it has a low-friction wear track. The MWCNT in the nanocomposites helped to maintain the hardness and strength of the nanocomposites at higher temperatures. Due to their high thermal conductivity, MWCNTs were able to help dissipate the heat generated during dry sliding conditions.

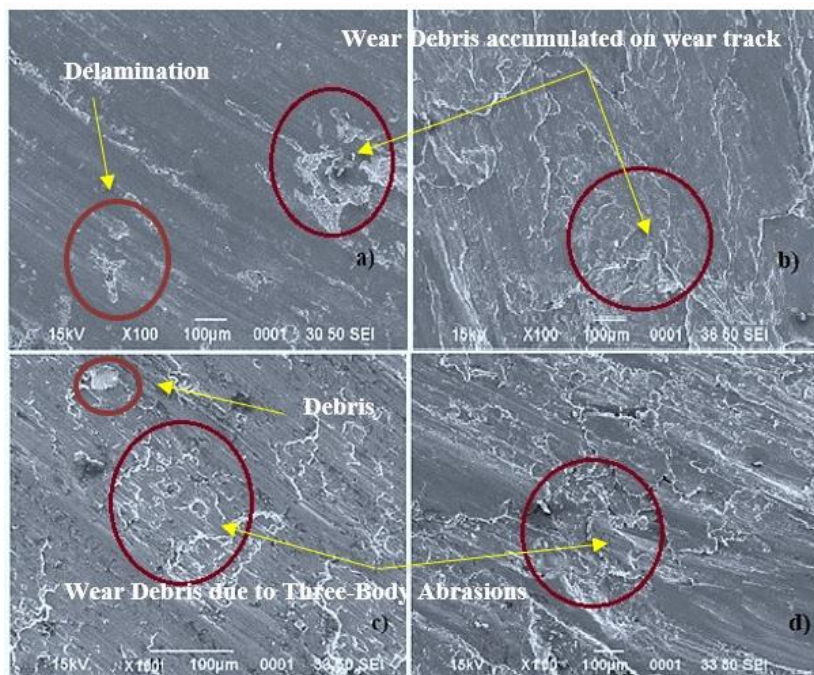


Figure 8. SEM Micrographs of Wear Tracks on Al-Si Coatings

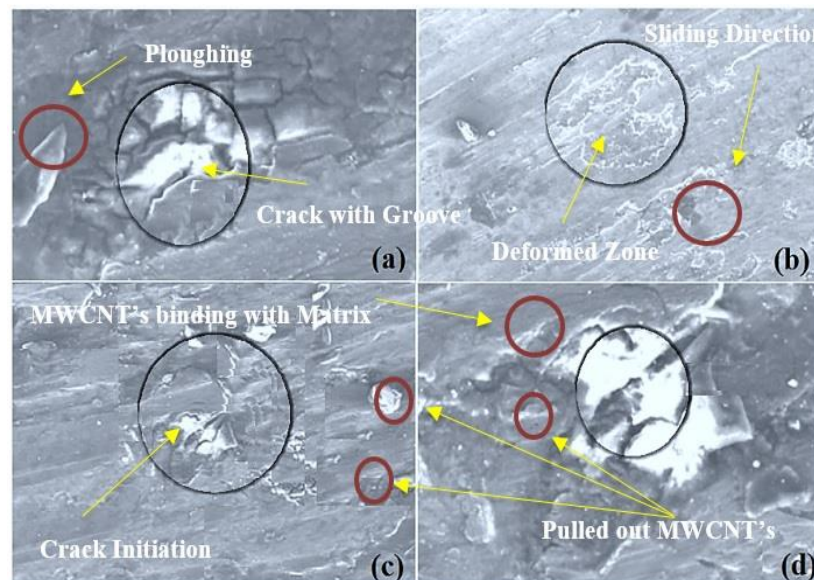


Figure 9. SEM micrographs of wear tracks on MWCNT-Al-Si composite coating

3.4. Results of Thermal conductivity

At room temperature, the thermal conductivity of LM6 coated Al-2024 was found to be slightly better than that of uncoated Al-2024, with a 2.1% increase. The thermal conductivity of Al-2024 was determined to be 127 ± 3.1 W/m-K, which is close to the reported value of 121 W/m-K. The experimental measurement of thermal conductivity for the Al-Si test block at room temperature was 138.27 ± 1.8 W/m-K. Therefore, the increase in thermal conductivity for LM6 coated Al-2024 can be attributed to the higher thermal conductivity of the coating. However, with increasing temperature, the thermal conductivity of uncoated Al-2024 improved, whereas the improvement in thermal conductivity of LM6 coated Al-2024 substrate was negligible. This can be explained by the fact that the thermal conductivity of the Al-Si test block also did not show significant improvement with increasing temperature. On the other hand, for the Al-2024 substrate coated with MWCNT reinforced Al-Si composite, there was a drastic improvement in thermal conductivity. Compared to LM6 coated Al-2024 and uncoated Al-2024, the thermal conductivity of the MWCNT-LM6 coating increased by 25% and 27% respectively. Figure 10 illustrates the thermal conductivities of the samples.

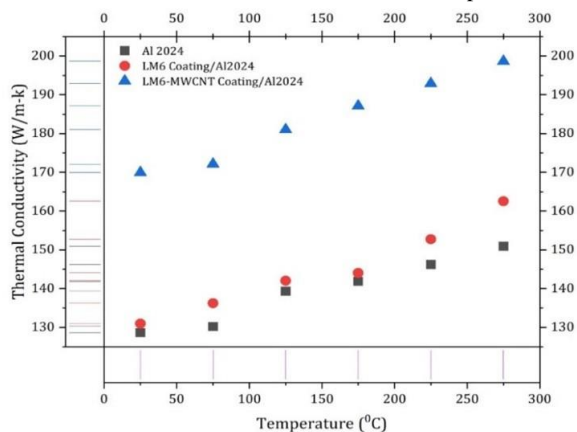


Figure 10. The thermal conductivity of MWCNT-LM6/Al and LM6/Al as a function of temperature

The thermal contact resistance at the MWCNT-LM6 coating and Al-2024 substrate could not be determined since free-standing MWCNT-Al-Si bulk structure could not be made. However, the thermal resistance at this interface should be lower due to the presence of MWCNTs at the interface, which is reflected by the improvement in thermal conductivity. Calculating thermal conductivity involves considering thermal diffusivity, specific heat capacity, and density. Thus, any enhancement in thermal conductivity can be attributed to an improvement in one or more of these factors or their combination. It was observed that due to the addition of MWCNTs, the thermal diffusivity of the Al-Si coated samples showed negligible improvement, whereas the density decreased.

4. CONCLUSION

Metal matrix composites (MMCs) incorporating carbon nanotubes (MWCNTs) as reinforcements have been successfully developed using the LENS (laser engineered net shaping) technique, which has led to enhanced properties of the composites.

- The addition of MWCNT to LM6 improved its wear resistance and led to a reduction in the coefficient of friction. Due to the addition of MWCNTs to LM6, its volumetric wear rate dropped by more than 90%. The

coefficient of friction decreased by almost 45%. This means that the MWCNTs can be added to metal matrices to improve their tribological properties.

- Coating Al-2024 substrate with LM6 led to a small improvement in its thermal conductivity. However, coating the substrate with the MWCNT- LM6 composite caused significant improvement in the thermal conductivity. This indicates higher thermal conductivity of the MWCNT-LM6 composite coatings. The high thermal conductivity of the MWCNT- LM6 is attributed to the improvement in specific heat caused by the addition of MWCNTs.
- The interface between the coating and the substrate exhibited very low thermal resistance due to the absence of a distinct boundary.

REFERENCES

- [1] Lakshmikanthan Avinash.; Angadi, S.; Malik, V.; Saxena, K.K.; Prakash, C.; Dixit, S.; Mohammed, K.A. (2022) "Mechanical and Tribological Properties of Aluminum-Based Metal-Matrix Composites". *Materials* 2022, 15, 6111. <https://doi.org/10.3390/ma15176111>.
- [2] Avinash Lakshmikanthan, Srikanth Bontha, M Krishna, Praveennath G Koppad, T Ramprabhu (2019) "Microstructure, mechanical and wear properties of the A357 composites reinforced with dual sized SiC particles" *Journal of Alloys and Compounds-Elsevier*, Volume 786, 25, Pp 570-580. <https://doi.org/10.1016/j.jallcom.2019.01.382>.
- [3] R. Banerjee; *Materials Science and Engineering A358* (2003) 343-349.
- [4] Vikram Kedambadi Vasu and Umashankar K S, "Experimental Investigation of Multi-Walled Carbon Nanotubes Dispersion on Mechanical Properties of Aluminum-Silicon Alloys (LM6 and LM25) by Stir Casting Method", *International Journal of Mechanical Engineering and Technology (IJMET)*, Volume: 8, Issue: 8, Pages: 341-348, 2017.
- [5] Shivalingaiah, K.; Nagarajaiah, V.; Selvan, C.P.; Kariappa, S.T.; Chandrashekarappa, N.G.; Lakshmikanthan, A.; Chandrashekarappa, M.P.G.; Linul, E. (2022) "Stir Casting Process Analysis and Optimization for Better Properties in Al-MWCNT-GR-Based Hybrid Composites". *Metals* 2022, 12, 1297. <https://doi.org/10.3390/met12081297>.
- [6] Manjunath Naik H R, Manjunath L H, Vinayak R. Malik, Manjunath Patel GC, Kuldeep K. Saxena & Avinash Lakshmikanthan (2021) "Effect of Microstructure, Mechanical and Wear on Al-CNTs/Graphene Hybrid MMCs". *Advances in Materials and Processing Technologies*, Taylor & Francis, DOI: 10.1080/2374068X.2021.1927646
- [7] Manjunath Naik H R, Manjunath L H, Vishwanath Koti, Avinash Lakshmikanthan, Praveennath G Koppad, Sampathkumaran P.: (2021), *Al/Graphene/CNT Hybrid Composites: Hardness and Sliding Wear Studies*, *FME Transactions* (2021) 49, 414-421. Doi: 10.5937/fme2102414N.
- [8] S.M. Zhou, X.B. Zhang, Z.P. Ding, C.Y. Min, G.L. Xu and W. M Zhu; "Composites A", 2007, 38A, 301-306.
- [9] Chu K, "Fabrication and effective thermal conductivity of multi-walled carbon nanotubes reinforced Cu matrix composites for heat sink applications", *Composites Science and Technology*, 2010.
- [10] R Banerjee, D Bhattacharyya, P.C Collins, G.B Viswanathan, H.L Fraser, "Precipitation of grain boundary α in a laser deposited compositionally graded Ti-8Al-xV alloy - an orientation microscopy study", *Acta Materialia*, 2004.
- [11] F Fisher, "Fiber waviness in nanotube-reinforced polymer composites - I: Modulus predictions using effective nanotube properties", *Composites Science and Technology*, 2003.
- [12] Kim, T. S, "Characterization of Ti-6Al-4V alloy modified by plasma carburizing process", *Materials Science & Engineering A*, 2003 1125.
- [13] Sudipto Chaki, Sujit Ghosal, "Chapter 1 LASOX Cutting: Principles and Evolution", Springer Science and Business Media LLC, 2019.

- [14] Nuno Silvestre, "Recent research and developments on the mechanical behavior of CNT-reinforced metal matrix composites", Walter de Gruyter GmbH, 2014.
- [15] Abhimanyu Bhat, Vamsi Krishna Balla, Sandip Bysakh, Debabrata Basu, Susmita Bose, Amit Bandyopadhyay. "Carbon nanotube reinforced Cu-10Sn alloy composites: Mechanical and thermal properties", *Materials Science and Engineering: A*, 2011.
- [16] Katrin I Schwendner, Rajarshi Banerjee, Peter C Collins, Craig A Brice, Hamish L Fraser. "Direct laser deposition of alloys from elemental powder blends", *Scripta Materialia*, 2001.
- [17] Anna Antolak-Dudka, Paweł Płatek, Tomasz Durejko, Paweł Baranowski, Jerzy Malachowski, Marcin Sarzynski and Tomasz Czujko, "Static and Dynamic Loading Behavior of Ti6Al4V Honeycomb Structures Manufactured by Laser Engineered Net Shaping (LENSTM) Technology", April 2019, *Materials* 12(1225):1-20.
- [18] J.Y. Hwang, A. Neira, T.W. Scharf, J. Tiley, R. Banerjee. "Laser-deposited carbon nanotube reinforced nickel matrix composites", *Scripta Materialia*, 2008.
- [19] S R Bakshi, D Lahiri, A Agarwal. "Carbon nanotube reinforced metal matrix composites – a review", *International Materials Reviews*, 2013.
- [20] B. Vamsi Krishna, Susmita Bose, Amit Bandyopadhyay. "Low stiffness porous Ti structures for load-bearing implants", *Acta Biomaterialia*, 2007.
- [21] Balla, V.K.. "Laser processed TiN reinforced Ti6Al4V composite coatings", *Journal of the Mechanical Behavior of Biomedical Materials*, 2012.
- [22] A. Wagih, A. Fathy. "Improving compressibility and thermal properties of Al-Al₂O₃ nanocomposites using Mg particles", *Journal of Materials Science*, 2018.
- [23] Nie X, "Tribological behaviour of oxide/graphite composite coatings deposited using electrolytic plasma process", *Surface & Coatings Technology*, 2004/11/12.
- [24] J. Castellon, H. Yahyaoui, O. Guille, E. David, M. Guo, M. Frechette. "Dielectric properties of POSS/LDPE and MgO/LDPE nanocomposites compounded by different techniques", 2017 IEEE Conference on Electrical Insulation and Dielectric Phenomenon (CEIDP), 2017.
- [25] Nagaraja S, Kodandappa R, Ansari K, Kuruniyan MS, Afzal A, Kaladgi AR, Aslfattahi N, Saleel CA, Gowda AC, Bindiganavile Anand P. Influence of Heat Treatment and Reinforcements on Tensile Characteristics of Aluminium AA 5083/Silicon Carbide/Fly Ash Composites. *Materials*. 2021; 14(18):5261
- [26] Bolzoni, L., M. Nowak, and N. Hari Babu. "Assessment of the influence of Al-2Nb-2B master alloy on the grain refinement and properties of LM6 (A413) alloy", *Materials Science and Engineering A*, 2015.
- [27] G. Madhu Sudana Reddy, C. Durga Prasad, Shanthala Kollur, A Lakshmikanthan, R. Suresh Kumar & C. R. Aprameya (2023) "Investigation of High-Temperature Erosion Behavior of NiCrAlY/TiO₂ Plasma Coatings on Titanium Substrate" *The Journal of The Minerals, Metals & Materials Society (TMS)*, Springer, Pp-1-7(2023).<https://doi.org/10.1007/s11837-023-05894-4>
- [28] Jiang L, "An approach to the uniform dispersion of a high-volume fraction of carbon nanotubes in aluminum powder", *Carbon*, 2011.
- [29] L. Zhou, T.B. Yuan, X.S. Yang, Z.Y. Liu, Q.Z. Wang, B.L. Xiao, Z.Y. Ma. "Micro-scale prediction of effective thermal conductivity of CNT/Al composites by finite element method", *International Journal of Thermal Sciences*, 2021.
- [30] B. Vamsi Krishna. "Fabrication of porous NiTi shape memory alloy structures using laser engineered net shaping", *Journal of Biomedical Materials Research Part B Applied Biomaterials*, 05/2009.
- [31] Abhimanyu Bhat, Vamsi Krishna Balla, Sandip Bysakh, Debabrata Basu, Susmita Bose, Amit Bandyopadhyay. "Carbon nanotube reinforced Cu-10Sn alloy composites: Mechanical and thermal properties", *Materials Science and Engineering: A*, 2011.
- [32] Balla, V K, "Direct laser processing of a tantalum coating on titanium for bone replacement structures", *Acta Biomaterialia*, 2010.
- [33] Padmakumar A. Bajakke, Vinayak R. Malik, Avinash L, Kuldeep K. Saxena & Anand S. Deshpande(2021) "A novel ultrahigh conductive Al-Cu composite produced via microwave sintering and post- treated by friction stir process". *Advances in Materials and Processing Technologies*, Taylor & Francis, DOI: 10.1080/2374068X.2021.1945270
- [34] Lulu Zhou, Henry Jay Forman, Yi Ge, Joseph Lunec. "Multi-walled carbon nanotubes: A cytotoxicity study in relation to functionalization, dose and dispersion", *Toxicology in Vitro*, 2017.
- [35] Bakshi, SR, "Aluminum composite reinforced with multiwalled carbon nanotubes from plasma spraying of spray dried powders", *Surface & Coatings Technology*, 2009.
- [36] Jin Lin, Haiyan Zhang, Haoqun Hong, Hui Liu, Xiubin Zhang. "A Thermally Conductive Composite with a Silica Gel Matrix and Carbon-Encapsulated Copper Nanoparticles as Filler", *Journal of Electronic Materials*, 2014.
- [37] Praveen KS, Shantharaja M, Manjunath Patel GC, Avinash L, Danil Yurievich P, Khaled Giasin and M Krishna "Corrosion Behaviour of High-Strength Al 7005 Alloy and Its Composites Reinforced with Industrial Waste-Based Fly Ash and Glass Fibre: Comparison of Stir Cast and Extrusion Conditions", *Materials*, - MDPI, 14(14), 3929, 2021. <https://doi.org/10.3390/ma14143929>
- [38] Sami Ullah, Faiz Ahmad, A.M. Shariff, M. Rafi Raza, Patrick J. Masset. "The role of multi-wall carbon nanotubes in char strength of epoxy-based intumescent fire-retardant coating", *Journal of Analytical and Applied Pyrolysis*, 2017.
- [39] N. Santhosh, N. Vinayaka, Aswatha, M. Uday, B.A. Praveena, Computational Analysis and Design for Precision Forging of Aluminium AA 6061 Connector, *Int. J. Comput. Eng. Res.* 3 (9) (2013) 1–8.
- [40] Moniruzzaman, M. "Increased flexural modulus and strength in SWNT/epoxy composites by a new fabrication method", *Polymer*, 2006.
- [41] L. Zhou, T.B. Yuan, X.S. Yang, Z.Y. Liu, Q.G. Wang, B.L. Xiao, Z.Y. Ma. "Micro-scale prediction of effective thermal conductivity of CNT/Al composites by finite element method", *International Journal of Thermal Sciences*, 2022
- [42] H.V. Moulya, A. Chandrashekar. "Experimental Investigation of Effect of Recycled Coarse Aggregate Properties on the Mechanical and Durability Characteristics of Geopolymer Concrete", *Materials Today: Proceedings*, 2022
- [43] Nagarajan T, C Pon Selvan, Avinash L, K Sivaprasad, B Ravisankar "Comparison based on specific strength and density of in-situ Ti/Al and Ti/Ni metal intermetallic laminates". *Journal of Materials Research and Technology-Elsevier*, Volume 14, Pp 1126-1136, ISSN 2238-7854, <https://doi.org/10.1016/j.jmrt.2021.06.102>
- [44] Avinash Lakshmikanthan, T Ramprabhu, Sai Babu Udayagiri, Praveenath G Koppad, Manoj Gupta, Krishna Munishamaiah, Srikanth Bontha (2020) "The effect of heat treatment on the mechanical and tribological properties of dual size SiC reinforced A357 matrix composites". *Journal of Materials Research and Technology-Elsevier*, 9(3), PP 6434-6452. <https://doi.org/10.1016/j.jmrt.2020.04.027>
- [45] Shiv Pratap Singh Yadav, Avinash Lakshmikanthan, Siddappa Ranganath, Manjunath Patel Gowdru Chandrashekarappa, Praveena Bindiganavile Anand, Vijay Kumar Shankar, Muralidhar Avvari, (2022) "Effect of Pin Geometry and Orientation on Friction and Wear Behavior of Nickel-Coated EN8 Steel Pin and Al6061 Alloy Disc Pair". vol. 2022, Article ID 3274672, PP-1-16, *Advances in Materials Science and Engineering*, -Hindawi, 14, 5095. <https://doi.org/10.1155/2022/3274672>
- [46] Rohith Sheshadri, Mohan Nagaraj, Avinash Lakshmikanthan, Manjunath Patel Gowdru Chandrashekarappa, Danil Yurievich Pimenov, Khaled Giasin, Raghupatruni Prasad, Szymon Wojciechowski (2021) "Experimental Investigation of Selective Laser Melting Parameters for Higher Surface Quality and Microhardness Properties: Taguchi and Super Ranking Concept Approaches". *Journal of Materials Research and Technology-*

- Elsevier. Volume 14, Pp 2586-2600, ISSN 2238-7854 <https://doi.org/10.1016/j.jmrt.2021.07.144>.
- [47] Vinayaka N, Avinash Lakshmikanthan, Manjunath Patel GC, Chithirai Pon Selvan, Vikram Kumar S Jain, S. A. Srinivasan & Harsha hm (2021) "Mechanical, Microstructure and Wear properties of Al 6113 Fly Ash reinforced Composites: Comparison of as cast and Heat-treated Conditions". *Advances-in Materials-and-Processing-Technologies*, -Taylor-&-Francis, DOI: 10.1080/2374068X.2021.1927649.
- [48] Shiv Pratap Singh Yadav, S. Ranganath, Salim Sharieff, R. Suresh, L. Avinash" (2020) "Investigations on the change in state of stress with respect to the sliding direction in dry sliding wear of hard elastic material with different geometry and orientation on ductile flat surface" *FME Transactions*, 48, 716-723. DOI: 10.5937/fme2003716S
- [49] Adithya Parthasarathy, Avinash L, Varun Kumar KN, Basavaraj Sajjan, Varun S (2017) "Fabrication and Characterization of Al-0.4%Si-0.5%Mg - SiCp using Permanent Mould Casting Technique" *Applied Mechanics and Materials*, Trans Tech Publications, Switzerland, ISSN: 1662-7482, Vol. 867, March 2017, pp 34-40, Doi: 10.4028/www.scientific.net/AMM.867.34
- [50] Basavaraj Sajjan, Avinash L, Varun, Varun Kumar KN, Adithya Parthasarathy (2017) "Investigation of Mechanical Properties and Dry Sliding Wear Behaviour of Graphite reinforced Al7068 alloy " *Applied Mechanics and Materials*, Trans Tech Publications, Switzerland, ISSN: 1662-7482, Vol. 867, March 2017, pp 10-18, Doi: 10.4028/www.scientific.net/AMM.867.10.
- [51] Yazan M. Almaetaha, Khaleel N. Abushgairb, Mohammad A. Hamdan, (2021) "Aluminium Alloys Nanostructures Produced by Accumulative Roll Bonding (ARB)", *Jordan Journal of Mechanical and Industrial Engineering*, Vol. 15 (4), pp 329-335.
- [52] Kiran Aithal S, Ramesh Babu N, Manjunath H N, Chethan K S, (2021) "Characterization of Al-SiCP Functionally Graded Metal Matrix Composites Developed through Centrifuge Casting Technique", *Jordan Journal of Mechanical and Industrial Engineering*, Vol. 15 (5), pp 483-490.
- [53] M. N. Abijitha, Adithya Rajeev Naira, M. Aadharsha, R. Vaira Vignesh R. Padmanaban, M. Arivarasub, (2018), "Investigations on the Mechanical, Wear and Corrosion Properties of Cold Metal Transfer Welded and Friction Stir Welded Aluminium Alloy AA2219", *Jordan Journal of Mechanical and Industrial Engineering*, Vol. 12 (4), pp 281-292.
- [54] Shashi Prakash Dwivedi, Rohit Sahu, (2018) "Effects of SiC Particles Parameters on the Corrosion Protection of Aluminum-based Metal Matrix Composites using Response Surface Methodology", *Jordan Journal of Mechanical and Industrial Engineering*, Vol. 12 (4), pp 313-321.
- [55] A. R. Nabillah, Z. Hamedon, M. T. Faiz, (2017) "Bits Reduction in the Electrodeposition Process of a Pickup Truck: a Case Study", *Jordan Journal of Mechanical and Industrial Engineering*, Vol. 11 (1), pp 27-33.
- [56] Ramadan J. Mustafa, (2010) "Abrasive Wear of Continuous Fibre Reinforced Al And Al-Alloy Metal Matrix Composites", *Jordan Journal of Mechanical and Industrial Engineering*, Vol. 4 (2), pp 246-255.
- [57] K. N. Abushgair, (2017) "Experimental Studies the Effect of Flap Peening Process on Aluminum Alloys", *Jordan Journal of Mechanical and Industrial Engineering*, Vol. 11 (3), pp 173-180.
- [58] Malek Ali, Samer Falih, (2014) "Synthesis and Characterization of Aluminum Composites Materials Reinforced with TiC Nano-Particles", *Jordan Journal of Mechanical and Industrial Engineering*, Vol. 8 (5), pp 257-264.
- [59] Shivaprasad Channappagoudar, Kiran Aithal, Narendranath Sannayallappa Vijay Desai, Pudukottah Gopalingar Mukundab, (2015) "The Influence of the Addition of 4.5 wt.% of Copper on Wear Properties of Al-12Si Eutectic Alloy", *Jordan Journal of Mechanical and Industrial Engineering*, Vol. 9 (3), pp 217-221.
- [60] A.R.I. Khedera ,G.S. Marahleh, D.M.K. Al-Jameaa, (2011) "Strengthening of Aluminum by SiC, Al₂O₃ and MgO", *Jordan Journal of Mechanical and Industrial Engineering*, Vol. 5 (6), pp 533-541.
- [61] S. Ezhil Vannan, S. Paul Vizhian, (2014), "Statistical Investigation on Effect of Electroless Coating Parameters on Coating Morphology of Short Basalt Fiber", *Jordan Journal of Mechanical and Industrial Engineering*, Vol. 8 (3), pp 153-160.
- [62] P.V.Chandra Sekhar Rao, A.Satya Devi, K.G.Basava Kumar, (2012) "Influence of Melt Treatments on Dry Sliding Wear Behavior of Hypereutectic Al-15Si-4Cu Cast Alloys", *JordanJournal of Mechanical and Industrial Engineering*, Vol. 6 (1), pp 55-61.
- [63] S. M. Al-Qawabah, (2012) "Effect of Direct Extrusion on the Microstructure, Microhardness, Surface Roughness and Mechanical Characteristics of Cu-Zn-Al Shape Memory Alloy, SMA", *JordanJournal of Mechanical and Industrial Engineering*, Vol. 6 (2), pp 171-181.
- [64] Ezhil Vannan, Paul Vizhian, (2015) "Corrosion Characteristics of Basalt Short Fiber Reinforced with Al-7075 Metal Matrix Composites", *JordanJournal of Mechanical and Industrial Engineering*, Vol. 9 (2), pp 121-128.
- [65] Lina M. Shehadeh, Issam S. Jalham, (2016) "The Effect of Adding Different Percentages of Manganese (Mn) and Copper (Cu) on the Mechanical Behavior of Aluminum", *JordanJournal of Mechanical and Industrial Engineering*, Vol. 10 (1), pp 19-26.
- [66] Ezhil Vannan, (2015) "Optimization of Coating Parameters on Coating Morphology of Basalt Short Fiber for Preparation of Al/Basalt Metal Matrix Composites Using Genetic Programming", *JordanJournal of Mechanical and Industrial Engineering*, Vol. 9 (1), pp 9-15.